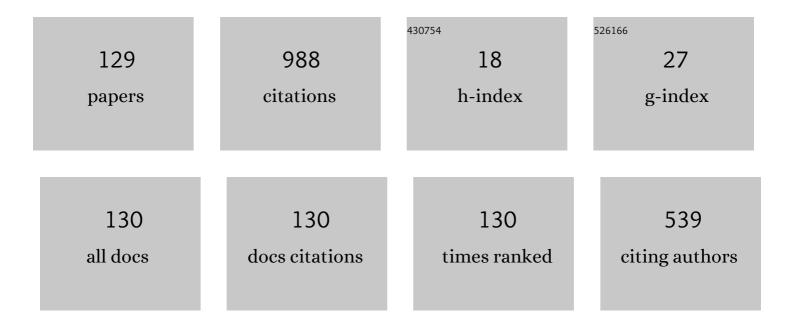
List of Publications by Year in descending order

Source: https://exaly.com/author-pdf/3351040/publications.pdf Version: 2024-02-01



#	Article	IF	CITATIONS
1	Gradient transition zone structure in "steel–copper―sample produced by double wire-feed electron beam additive manufacturing. Journal of Materials Science, 2020, 55, 9258-9272.	1.7	62
2	The strain-rate dependence of the Hall-Petch effect in two austenitic stainless steels with different stacking fault energies. Materials Science & Engineering A: Structural Materials: Properties, Microstructure and Processing, 2019, 756, 365-372.	2.6	58
3	Hydrogen-induced twinning in 〈001〉 Hadfield steel single crystals. Scripta Materialia, 2010, 63, 1189-119	22.6	46
4	Microstructure and grain growth inhomogeneity in austenitic steel produced by wire-feed electron beam melting: the effect of post-building solid-solution treatment. Journal of Materials Science, 2020, 55, 9211-9224.	1.7	41
5	Phase Composition of Austenitic Stainless Steels in Additive Manufacturing: A Review. Metals, 2021, 11, 1052.	1.0	40
6	Annealing behavior of ultrafine grained structure in low-carbon steel produced by equal channel angular pressing. Materials Science & Engineering A: Structural Materials: Properties, Microstructure and Processing, 2013, 581, 104-107.	2.6	37
7	Microstructure and mechanical response of single-crystalline high-manganese austenitic steels under high-pressure torsion: The effect of stacking-fault energy. Materials Science & Engineering A: Structural Materials: Properties, Microstructure and Processing, 2014, 604, 166-175.	2.6	33
8	The role of twinning on microstructure and mechanical response of severely deformed single crystals of high-manganese austenitic steel. Materials Characterization, 2011, 62, 588-592.	1.9	30
9	Hydrogen Embrittlement of Austenitic Stainless Steels with Ultrafine-Grained Structures of Different Morphologies. Physical Mesomechanics, 2019, 22, 313-326.	1.0	27
10	On the difference in carbon- and nitrogen-alloying of equiatomic FeMnCrNiCo high-entropy alloy. Materials Letters, 2020, 276, 128183.	1.3	26
11	The effect of nitrogen alloying on hydrogen-assisted plastic deformation and fracture in FeMnNiCoCr high-entropy alloys. Scripta Materialia, 2021, 194, 113642.	2.6	24
12	Influence of equal-channel angular pressing on the structure and mechanical properties of low-carbon steel 10G2FT. Physics of Metals and Metallography, 2010, 110, 260-268.	0.3	20
13	Microstructure of EK-181 ferritic-martensitic steel after heat treatment under various conditions. Technical Physics, 2012, 57, 48-54.	0.2	20
14	Thermal stability of the microstructure of 12% chromium ferritic–martensitic steels after long-term aging at high temperatures. Technical Physics, 2016, 61, 209-214.	0.2	20
15	Peculiarities of Structure Formation in Copper/Steel Bimetal Fabricated by Electron-Beam Additive Technology. Russian Physics Journal, 2019, 62, 1486-1494.	0.2	20
16	Low-temperature tensile ductility by V-alloying of high-nitrogen CrMn and CrNiMn steels: Characterization of deformation microstructure and fracture micromechanisms. Materials Science & Engineering A: Structural Materials: Properties, Microstructure and Processing, 2019, 745, 265-278.	2.6	20
17	Structure and mechanical properties of low-carbon ferrite-pearlite steel after severe plastic deformation and subsequent high-temperature annealing. Physical Mesomechanics, 2011, 14, 195-203.	1.0	19
18	The microstructure, phase composition and tensile properties of austenitic stainless steel in a wire-feed electron beam melting combined with ultrasonic vibration. Materials Science & Engineering A: Structural Materials: Properties, Microstructure and Processing, 2021, 820, 141519.	2.6	19

#	Article	IF	CITATIONS
19	The effect of solid-solution temperature on phase composition, tensile characteristics and fracture mechanism of V-containing CrMn-steels with high interstitial content C+N>1 mass. %. Materials Science & amp; Engineering A: Structural Materials: Properties, Microstructure and Processing, 2020, 770, 138534.	2.6	18
20	The influence of orientation and aluminium content on the deformation mechanisms of Hadfield steel single crystals. International Journal of Materials Research, 2007, 98, 144-149.	0.1	17
21	Structural and phase transformations in nanostructured 0.1% C-Mn-V-Ti steel during cold deformation by high pressure torsion and subsequent heating. Nanotechnologies in Russia, 2009, 4, 109-120.	0.7	17
22	High-Strength Single Crystals of Austenitic Stainless Steels with Nitrogen Content: Mechanisms of Deformation and Fracture. Materials Science Forum, 1999, 318-320, 395-400.	0.3	16
23	A comparative study of a solid solution hardening in carbon-alloyed FeMnCrNiCo0.95C0.05 high-entropy alloy subjected to different thermal–mechanical treatments. Materials Letters, 2021, 285, 129073.	1.3	16
24	Structure–phase transformations and physical properties of ferritic–martensitic 12% chromium steels EK-181 and ChS-139. Technical Physics, 2016, 61, 97-102.	0.2	15
25	Anisotropy of the tensile properties in austenitic stainless steel obtained by wire-feed electron beam additive growth. Letters on Materials, 2019, 9, 460-464.	0.2	15
26	Stabilization of austenitic structure in transition zone of "austenitic stainless steel/NiCr alloy―joint fabricated by wire-feed electron beam melting. Materials Letters, 2020, 277, 128321.	1.3	14
27	The effect of heat treatment on the microstructure and mechanical properties of heat-resistant ferritic–martensitic steel EK-181. Journal of Nuclear Materials, 2014, 455, 665-668.	1.3	13
28	Electron-beam additive manufacturing of high-nitrogen steel: Microstructure and tensile properties. Materials Science & Engineering A: Structural Materials: Properties, Microstructure and Processing, 2021, 826, 141951.	2.6	13
29	The effect of aluminum alloying on ductile-to-brittle transition in Hadfield steel single crystal. International Journal of Fracture, 2009, 160, 143-149.	1.1	12
30	Comparative study of shock-wave hardening and substructure evolution of 304L and Hadfield steels irradiated with a nanosecond relativistic high-current electron beam. Journal of Alloys and Compounds, 2017, 714, 232-244.	2.8	11
31	Hydrogen-enhanced orientation dependence of stress relaxation and strain-aging in Hadfield steel single crystals. Scripta Materialia, 2017, 136, 101-105.	2.6	11
32	The effect of age-hardening mechanism on hydrogen embrittlement in high-nitrogen steels. International Journal of Hydrogen Energy, 2019, 44, 20529-20544.	3.8	11
33	A role of initial microstructure in characteristics of the surface layers produced by ion-plasma treatment in CrNiMo austenitic stainless steel. Materials Characterization, 2019, 153, 372-380.	1.9	11
34	Advanced high-strength AA5083 welds by high-speed hybrid laser-arc welding. Materials Letters, 2021, 291, 129594.	1.3	10
35	Shape memory effects in FeNiCoTi single crystals undergoing γ ↔ α′ thermoelastic martensitic transformations. Doklady Physics, 2004, 49, 47-50.	0.2	9
36	The influence of intergranular and interphase boundaries and δferrite volume fraction on hydrogen embrittlement of high-nitrogen steel. International Journal of Hydrogen Energy, 2021, 46, 30510-30522.	3.8	9

#	Article	IF	CITATIONS
37	Microstructure and mechanical properties of Nb-alloyed austenitic CrNi steel fabricated by wire-feed electron beam additive manufacturing. Materials Characterization, 2022, 190, 112063.	1.9	9
38	Microstructural Characterization of Low-Carbon Steel Processed by High Pressure Torsion and Annealing. Materials Science Forum, 2008, 584-586, 649-654.	0.3	7
39	feaagaart1ev2aaatCvAufeBSjuy2L2yd9g2LbvyNv2CaerbuLwBLn % hiov2DGi1BTfMBaeXatLxBI9gBaerbd9wDYLwzYbltLDharqqtubsr % 4rNCHbGeaGqiVu0Je9sqqrpepC0xbbL8F4rqqrFfpeea0xe9Lq-Jc9 % vqaqpepm0xbba9pwe9Q8fs0-yqaqpepae9pg0FirpepeKkFr0xfr-x %	0.3	7
40	The effect of tempering temperature on the features of phase transformations in the ferritic–martensitic steel EK-181. Journal of Nuclear Materials, 2014, 455, 496-499.	1.3	7
41	Effect of hydrogenation on mechanical properties and tensile fracture mechanism of a high-nitrogen austenitic steel. Journal of Materials Science, 2017, 52, 4224-4233.	1.7	7
42	Stable high-nickel austenitic steel produced by electron beam additive manufacturing using dual wire-feed system. Materials Letters, 2021, 305, 130863.	1.3	7
43	Temperature Dependence of Mechanical Properties and Plastic Flow Behavior of Cast Multicomponent Alloys Fe20Cr20Mn20Ni20Co20-xCx (x = 0, 1, 3, 5). Physical Mesomechanics, 2021, 24, 674-683.	1.0	7
44	Deformation mechanisms and strain hardening of Hadfield-steel single crystals alloyed with aluminum. Doklady Physics, 2002, 47, 515-517.	0.2	6
45	The Effect of Heat-Treatment Modes on Microstructure of Reduced-Activation Ferritic-Martensitic Steel EK-181. Russian Physics Journal, 2013, 56, 542-545.	0.2	6
46	The Effect of Test Temperature on Deformation Microstructure and Fracture Mechanisms in CrMn High-Nitrogen Steels Alloyed (0-3 wt.%) with Vanadium. Materials Science Forum, 2018, 941, 27-32.	0.3	6
47	Effect of Ion-Plasma Nitriding on Phase Composition and Tensile Properties of AISI 321-Type Stainless Steel Produced by Wire-Feed Electron-Beam Additive Manufacturing. Metals, 2022, 12, 176.	1.0	5
48	The influence of severe plastic deformation by high pressure torsion on structure and mechanical properties of Hadfield steel single crystals. Journal of Physics: Conference Series, 2010, 240, 012139.	0.3	4
49	Effect of high-temperature annealing on the microstructure and mechanical properties of ferritic-pearlitic steel 10G2FT subjected to equal-channel angular pressing. Physics of Metals and Metallography, 2011, 111, 62-71.	0.3	4
50	Structural features and mechanical properties of austenitic Hadfield steel after high-pressure torsion and subsequent high-temperature annealing. Physics of Metals and Metallography, 2012, 113, 612-620.	0.3	4
51	The influence of temperature on microstructure and microhardness in high-pressure torsion of low-carbon steel. IOP Conference Series: Materials Science and Engineering, 2014, 63, 012133.	0.3	4
52	Hydrogen Embrittlement of Ultrafine-Grained Austenitic Stainless Steels. Reviews on Advanced Materials Science, 2018, 54, 25-45.	1.4	4
53	Effect of Hydrogen Charging on Mechanical Twinning, Strain Hardening, and Fracture of â€1111› and â€1144â€ Hadfield Steel Single Crystals. Physical Mesomechanics, 2018, 21, 263-273.	<sup>€⁰</sup> 1.0	4
54	Effect of Grain Refinement on the Elemental Composition and Nanohardness of the Surface Layers in AISI 316L Austenitic Steel Subjected to Ion-Plasma Hardening. Defect and Diffusion Forum, 0, 385, 267-272.	0.4	4

EG ASTAFUROVA

#	Article	IF	CITATIONS
55	Microstructural inhomogeneity of phase composition and grain structure in electron beam wire-feed additive manufactured AISI 304 stainless steel. AIP Conference Proceedings, 2019, , .	0.3	4
56	A Comparison of Strengthening Mechanisms of Austenitic Fe-13Mn-1.3C Steel in Warm and Cold High-Pressure Torsion. Metals, 2020, 10, 493.	1.0	4
57	The effect of thin surface layer of nitrogen-expanded austenite on bulk γ-α' phase transformation in low-temperature deformation of 316L stainless steel. Materials Letters, 2021, 304, 130676.	1.3	4
58	THE EFFECT OF NIOBIUM ON MICROSTRUCTURE AND MECHANICAL PROPERTIES OF AUSTENITIC CrNi STEEL PRODUCED BY WIRE-FEED ELECTRON BEAM ADDITIVE MANUFACTURING. Nanoscience and Technology, 2020, 11, 109-118.	0.6	4
59	Grain refinement and mechanical properties of low-carbon steel by means of equal channel angular pressing and annealing. International Journal of Materials Research, 2013, 104, 457-461.	0.1	3
60	Influence of rolling temperature on structure, phase composition and mechanical properties of austenitic steel Fe–17Cr–13Ni–3Mo. AlP Conference Proceedings, 2015, , .	0.3	3
61	The Influence of the Thermomechanical Processing Regime on the Structural Evolution of Mo-Nb-Ti-V Microalloyed Steel Subjected to High-Pressure Torsion. Metallurgical and Materials Transactions A: Physical Metallurgy and Materials Science, 2017, 48, 3400-3409.	1.1	3
62	Effect of vanadium-alloying on hydrogen embrittlement of austenitic high-nitrogen steels. Procedia Structural Integrity, 2018, 13, 1053-1058.	0.3	3
63	Effect of stacking fault energy on Hall–Petch relationship parameters of austenitic stainless steels. AIP Conference Proceedings, 2019, , .	0.3	3
64	On the Superplastic Deformation in Vanadium-Alloyed High-Nitrogen Steel. Metals, 2020, 10, 27.	1.0	3
65	The effect of hydrogen alloying on strain hardening and fracture of a high-nitrogen austenitic steel. Letters on Materials, 2018, 8, 71-76.	0.2	3
66	Microstructure and mechanical properties of low-carbon steel fabricated by electron-beam additive manufacturing. Letters on Materials, 2021, 11, 427-432.	0.2	3
67	Strain localization in <111> single crystals of Hadfield steel under compressive load. Journal of Physics: Conference Series, 2010, 240, 012018.	0.3	2
68	The microstructural stability of low-activation 12%-chromium ferritic-martensitic steel EK-181 during thermal aging. AIP Conference Proceedings, 2014, , .	0.3	2
69	The effect of hydrogen on strain hardening and fracture mechanism of high-nitrogen austenitic steel. IOP Conference Series: Materials Science and Engineering, 2016, 140, 012005.	0.3	2
70	Microhardness homogeneity and microstructure of high-nitrogen austenitic steel processed by high-pressure torsion. AIP Conference Proceedings, 2017, , .	0.3	2
71	A comparative study of the macroscopical and microscopical fracture mechanisms in cast and additively manufactured austenitic stainless steels. AIP Conference Proceedings, 2019, , .	0.3	2
72	The Influence of Phase Composition and Phase Distribution on Crack Formation and Fracture Mechanisms of Cr–Ni Steels Produced by the Method of 3D Electron-Beam Printing. Russian Physics Journal, 2020, 63, 917-925.	0.2	2

#	Article	IF	CITATIONS
73	On Temperature Dependence of Microstructure, Deformation Mechanisms and Tensile Properties in Austenitic Cr-Mn Steel with Ultrahigh Interstitial Content C + N = 1.9 Mass.%. Metals, 2020, 10, 786.	1.0	2
74	The Effect of Hydrogen-Charging on Mechanical Properties of Austenitic CrNi Steel Fabricated by Wire-Feed Electron Beam Additive Manufacturing. E3S Web of Conferences, 2021, 225, 01011.	0.2	2
75	Effect of annealing in the range of thermal stability on structure peculiarities of steel Fe-Mo-Nb-V-0.08C processed by high-pressure torsion. Letters on Materials, 2015, 5, 432-436.	0.2	2
76	Microstructure and phase composition of vanadium-alloyed high-nitrogen steel fabricated by additive manufacturing. AIP Conference Proceedings, 2020, , .	0.3	2
77	The Effect of Phase Transformations During Electrom-Beam 3D-Printing and Post-Built Heat Treatment on Plastic Deformation and Fracture of Additively Manufactured High Nitrogen Cr–Mn Steel. Russian Physics Journal, 2021, 64, 1183-1190.	0.2	2
78	Shape memory effect and superelasticity in single-phase nickel titanium single crystals. European Physical Journal Special Topics, 2004, 115, 175-183.	0.2	1
79	The effect of aluminium on mechanical properties and deformation mechanisms of hadfield steel single crystals. European Physical Journal Special Topics, 2004, 115, 243-250.	0.2	1
80	Ductile-to-Brittle transition in 〈111〉 hadfield steel single crystals. Russian Metallurgy (Metally), 2010, 2010, 857-861.	0.1	1
81	The Evolution of Structure and Mechanical Properties of Fe-Mn-V-Ti-0,1C Low-Carbon Steel Subjected to Severe Plastic Deformation and Subsequent Annealing. Materials Science Forum, 2010, 667-669, 325-330.	0.3	1
82	The Evolution of Structure and Mechanical Properties of Fe-Mn-V-Ti-0,1C Low-Carbon Steel Subjected to Severe Plastic Deformation and Subsequent Annealing. Materials Science Forum, 0, 715-716, 994-999.	0.3	1
83	The influence of heat treatment on homogeneity of strength properties and structural peculiarities of low-carbon steel Fe-Mo-Nb-V-C processed by high-pressure torsion. , 2014, , .		1
84	Thermal stability of nanostructured Hadfield steel produced by high-pressure torsion. , 2014, , .		1
85	Microstructure and mechanical properties of heat-resistant 12% Cr ferritic-martensitic steel EK-181 after thermomechanical treatment. AIP Conference Proceedings, 2015, , .	0.3	1
86	Structure, phase composition and mechanical properties of austenitic steel Fe–18Cr–9Ni–0.5Ti–0.08C subjected to chemical-deformation processing. AlP Conference Proceedings, 2016, , .	0.3	1
87	Influence of hydrogenation regime on structure, phase composition and mechanical properties of Fe18Cr9Ni0.5Ti0.08C steel in cold rolling. AIP Conference Proceedings, 2017, , .	0.3	1
88	Temperature Dependence of Tensile Deformation and Fracture Micromechanisms in V-Alloyed High-Nitrogen Steel: Effect of Solution-Treatment Temperature. Procedia Structural Integrity, 2018, 13, 1129-1134.	0.3	1
89	Influence of hydrogen-charging on microstructure and microhardness of high-nitrogen austenitic steel processed by high-pressure torsion. AIP Conference Proceedings, 2018, , .	0.3	1
90	The Influence of Warm abc-Pressing on the Structure and Mechanical Properties of Stable Chromium-Nickel-Molybdenum Steel. Russian Physics Journal, 2018, 61, 1062-1069.	0.2	1

#	Article	IF	CITATIONS
91	Effect of annealing on microhardness and phase composition of high-manganese austenitic steels with twinning-associated microstructures produced by high-pressure torsion. AIP Conference Proceedings, 2019, , .	0.3	1
92	On the influence of post-built heat treatment on strength and ductility of AISI 304 steel produced by electron-beam additive technology. AIP Conference Proceedings, 2019, , .	0.3	1
93	The Effect of Thermo-Mechanical Processing Regime on High-Temperature Tensile Properties of V-Alloyed High-Nitrogen Steel. Solid State Phenomena, 2020, 306, 53-61.	0.3	1
94	The grain size-dependent control of the phase composition in ion-plasma treated 316L stainless steel. Materials Science & Engineering A: Structural Materials: Properties, Microstructure and Processing, 2021, 823, 141777.	2.6	1
95	The effect of high-pressure torsion on microstructure and strength properties of high-nitrogen austenitic steel. Letters on Materials, 2014, 4, 269-272.	0.2	1
96	The influence of prior deformation on phase composition and strength properties of austenitic stainless steel in ion-plasma treatment. Letters on Materials, 2019, 9, 377-381.	0.2	1
97	Effect of deformation temperature on the structural parameters, phase composition and microhardness of Fe-28Mn-2.7Al-1.3C steel single crystals processed by high-pressure torsion. Letters on Materials, 2018, 8, 178-183.	0.2	1
98	Influence of Hydrogen-Charging Regime on Strain Hardening and Deformation Mechanism of Hot-Rolled High-Nitrogen Austenitic Steel. Acta Physica Polonica A, 2018, 134, 760-764.	0.2	1
99	Microstructure and phase composition of high-nitrogen steel fabricated by electron beam additive manufacturing. AIP Conference Proceedings, 2020, , .	0.3	1
100	Influence of thermal and thermal-mechanical treatments on microstructure and mechanical properties of the multicomponent alloy FeCrMnNiCo0.85C0.15. Letters on Materials, 2021, 11, 375-381.	0.2	1
101	Mechanical properties and fracture behavior of ferritic-perlitic steel Fe-Mn-V-Ti-C subjected to equal channel angular pressing and high-temperature annealing. Inorganic Materials: Applied Research, 2011, 2, 370-376.	0.1	0
102	The effect of hydrogenation on structure and strength properties of austenitic stainless steel Fe-18Cr-9Ni-Ti. , 2014, , .		0
103	The effect of severe plastic deformation by high-pressure torsion on structure and phase composition of high-nitrogen austenitic steel. AIP Conference Proceedings, 2015, , .	0.3	0
104	The effect of hydrogenation on strain hardening and deformation mechanisms in ã€^113〉 single crystals of Hadfield steel. AIP Conference Proceedings, 2015, , .	0.3	0
105	The influence of initial heat treatment of low-carbon steel Fe-Mo-Nb-V-C on peculiarities of ultrafine-grained structure in high-pressure torsion. AIP Conference Proceedings, 2015, , .	0.3	0
106	Microstructural features and microhardness of Fe-Mo-Nb-V-C low-carbon steel processed by high-pressure torsion: The significance of the initial structural state. AIP Conference Proceedings, 2016, , .	0.3	0
107	Evolution of grain–subgrain structure and carbide subsystem upon annealing of a low-carbon low-alloy steel subjected to high-pressure torsion. Physics of Metals and Metallography, 2016, 117, 1101-1110.	0.3	0
108	Strain hardening and fracture behavior during tension of directionally solidified high-nitrogen austenitic steel. AIP Conference Proceedings, 2017, , .	0.3	0

#	Article	IF	CITATIONS
109	Influence of thermomechanical treatments on mechanical properties and fracture mechanism of high-nitrogen austenitic steel. AIP Conference Proceedings, 2017, , .	0.3	0
110	Effect of rolling on phase composition and microhardness of austenitic steels with different stacking-fault energies. AIP Conference Proceedings, 2017, , .	0.3	0
111	The effect of solution treatment regime on temperature dependence of 0.2% offset yield strength in V-alloyed high-nitrogen austenitic steel. AIP Conference Proceedings, 2018, , .	0.3	0
112	Effect of age hardening on phase composition and microhardness of V-free and V-alloyed high-nitrogen austenitic steels. AIP Conference Proceedings, 2018, , .	0.3	0
113	The effect of solid-solution temperature on phase composition and tensile properties of vanadium-alloyed high interstitial steels. AIP Conference Proceedings, 2019, , .	0.3	0
114	Influence of hydrogen saturation on the structure and mechanical properties of Fe-17Cr-13Ni-3Mo-0.01C austenitic steel during rolling at different temperatures. Metal Working and Material Science, 2021, 23, 81-97.	0.0	0
115	Effect of electrolytic hydrogen saturation on deformation mechanisms of Fe-17Cr-13Ni-3Mo-0.01C austenitic stainless steel during cold rolling. Letters on Materials, 2021, 11, 285-290.	0.2	0
116	Influence of ion nitriding regime on mechanical properties and fracture mechanism of austenitic steel subjected to different thermomechanical treatments. AIP Conference Proceedings, 2016, , .	0.3	0
117	Hydrogen-Assisted Fracture Mechanisms in Ultrafine-Grained CrNi Austenitic Stainless Steels with Different Initial Microstructures. Materials Science Forum, 0, 941, 370-375.	0.3	0
118	The effect of hydrogen charging on the mechanical properties and fracture mechanisms of high-nitrogen chromium-manganese steels after age-hardening. Vektor Nauki Tol Yattinskogo Gosudarstvennogo Universiteta, 2020, , 57-67.	0.1	0
119	The influence of age hardening on microstructure, phase composition, and microhardness of high-nitrogen austenitic steel. Vektor Nauki Tol Yattinskogo Gosudarstvennogo Universiteta, 2020, , 74-81.	0.1	0
120	On the influence of strain rate and deformation temperature on the peculiarities of plastic flow in vanadium-alloyed austenitic steel with high interstitial content. AIP Conference Proceedings, 2020, , .	0.3	0
121	Mechanical properties and fracture micromechanisms in 316L stainless steel subjected to ion-plasma treatment with mixture of N, H and Ar gases. AIP Conference Proceedings, 2020, , .	0.3	0
122	The change in solidification mode and phase composition in "321 stainless Steel/NiCr Alloy―joint produced by Wire-feed electron beam melting. AIP Conference Proceedings, 2020, , .	0.3	0
123	The peculiarities of hydrogen embrittlement of Nb-alloyed stainless steel fabricated by electron-beam additive manufacturing. AIP Conference Proceedings, 2020, , .	0.3	0
124	Peculiarities of tensile deformation and fracture of high-nitrogen steel obtained by electron beam additive manufacturing. AIP Conference Proceedings, 2020, , .	0.3	0
125	Effect of the precipitation hardening on regularities of plastic deformation and fracture mode of V-alloyed high nitrogen austenitic steel. Vektor Nauki Tol Yattinskogo Gosudarstvennogo Universiteta, 2020, , 42-50.	0.1	0
126	Microstructure/mechanical properties relationship in high-nitrogen steel obtained by electron beam additive manufacturing and conventional casting. AIP Conference Proceedings, 2020, , .	0.3	0

#	Article	IF	CITATIONS
127	Hydrogen embrittlement of the additively manufactured Nb-free and Nb-alloyed austenitic steels. AIP Conference Proceedings, 2022, , .	0.3	0
128	Thermo-Mechanical Processing and Additive Manufacturing of Steels. Metals, 2022, 12, 731.	1.0	0
129	Microstructural effect on hydrogen embrittlement of high nitrogen chromium-manganese steel. , 2022, 25, 84-97.		0